

Biological Low-pH Mn(II) Oxidation in a Manganese Deposit Influenced by Metal-Rich Groundwater

Tsing Bohu,^a Denise M. Akob,^b Michael Abratis,^c Cassandre S. Lazar,^a Kirsten Küsel^{a,d}

Aquatic Geomicrobiology, Institute of Ecology, Friedrich Schiller University Jena, Jena, Germany^a; U.S. Geological Survey, National Research Program, Reston, Virginia, USA^b; Institute of Geosciences, Friedrich Schiller University Jena, Jena, Germany^c; German Centre for Integrative Biodiversity Research (iDiv) Halle-Jena-Leipzig, Leipzig, Germany^d

ABSTRACT

The mechanisms, key organisms, and geochemical significance of biological low-pH Mn(II) oxidation are largely unexplored. Here, we investigated the structure of indigenous Mn(II)-oxidizing microbial communities in a secondary subsurface Mn oxide deposit influenced by acidic (pH 4.8) metal-rich groundwater in a former uranium mining area. Microbial diversity was highest in the Mn deposit compared to the adjacent soil layers and included the majority of known Mn(II)-oxidizing bacteria (MOB) and two genera of known Mn(II)-oxidizing fungi (MOF). Electron X-ray microanalysis showed that romanecchite [(Ba₂H₂O)₂(Mn⁴⁺, Mn³⁺)₅O₁₀] was conspicuously enriched in the deposit. Canonical correspondence analysis revealed that certain fungal, bacterial, and archaeal groups were firmly associated with the autochthonous Mn oxides. Eight MOB within the *Proteobacteria*, *Actinobacteria*, and *Bacteroidetes* and one MOF strain belonging to *Ascomycota* were isolated at pH 5.5 or 7.2 from the acidic Mn deposit. Soil-groundwater microcosms demonstrated 2.5-fold-faster Mn(II) depletion in the Mn deposit than adjacent soil layers. No depletion was observed in the abiotic controls, suggesting that biological contribution is the main driver for Mn(II) oxidation at low pH. The composition and species specificity of the native low-pH Mn(II) oxidizers were highly adapted to *in situ* conditions, and these organisms may play a central role in the fundamental biogeochemical processes (e.g., metal natural attenuation) occurring in the acidic, oligotrophic, and metalliferous subsoil ecosystems.

IMPORTANCE

This study provides multiple lines of evidence to show that microbes are the main drivers of Mn(II) oxidation even at acidic pH, offering new insights into Mn biogeochemical cycling. A distinct, highly adapted microbial community inhabits acidic, oligotrophic Mn deposits and mediates biological Mn oxidation. These data highlight the importance of biological processes for Mn biogeochemical cycling and show the potential for new bioremediation strategies aimed at enhancing biological Mn oxidation in low-pH environments for contaminant mitigation.

Biogenic Mn oxides contribute to the natural attenuation of metals, providing a potentially ecologically and economically friendly strategy for the *in situ* stabilization of metal pollutants in natural ecosystems and anthropogenic settings (1, 2). The pH of environments that would be good targets for Mn oxide-mediated attenuation, e.g., drainage basins, mine tailings, and leaching heaps, is normally acidic due to the aerobic oxidation of sulfidic minerals (3). Although manganese is readily oxidized from Mn(II) to Mn(III/IV) at circumneutral pH by a variety of microorganisms (4), we have limited knowledge about the formation of biogenic Mn oxides in acidic environments (5, 6).

In natural environments with pH values from 6 to 8.5 and oxidic conditions, the occurrence of Mn oxides is mainly due to biological contributions (7). Diverse microorganisms, both prokaryotes and eukaryotes, are capable of oxidizing Mn(II) ions at circumneutral pH (8–10). Mn(II)-oxidizing bacteria (MOB) include *Roseobacter* sp. strain AzwK-3b (11), *Bacillus* sp. strain SG-1 (12), *Leptothrix* sp. (13), *Pseudomonas putida* GB-1 (14), and *Aurantimonas manganooxydans* (15), which are found in the *Proteobacteria*, *Firmicutes*, and *Actinobacteria* phyla. *Crenarchaeota*, the most abundant archaea in marine environments known to be involved in chemoautotrophic nitrification (16) are closely associated with Mn oxides in freshwater (17), although it has not been definitively shown to oxidize Mn in the laboratory. Several fungal species be-

longing to the phyla of *Ascomycota* and *Basidiomycota* have also been identified as Mn(II)-oxidizing fungi (MOF) (8, 18).

In contrast, low-pH Mn(II) oxidation poses a challenge to microbes because the reaction is thermodynamically unfavored (5, 6, 19, 20). Until recently, only the fungus *Cephalosporium* sp. and cell extracts of *Streptomyces* spp. were reported to be able to oxidize Mn(II) at pH values below 5 (21, 22). However, recently, Akob et al. reported new isolates of low-pH MOB, including *Duganella* sp. strain AB_14 and *Albidiferax ferrireducens* strain TB-2, which oxidize Mn(II) at pH 5.5 (5). In addition, Bohu et al. characterized *Mesorhizobium australicum* T-G1, a low-pH Mn(II) oxidizer, that forms a bixbyite-like phase via a multi-copper oxidase pathway rather than reactive oxygen species at acidic pH (6).

Received 26 November 2015 Accepted 4 March 2016

Accepted manuscript posted online 11 March 2016

Citation Bohu T, Akob DM, Abratis M, Lazar CS, Küsel K. 2016. Biological low-pH Mn(II) oxidation in a manganese deposit influenced by metal-rich groundwater. *Appl Environ Microbiol* 82:3009–3021. doi:10.1128/AEM.03844-15.

Editor: S.-J. Liu, Chinese Academy of Sciences

Address correspondence to Kirsten Küsel, kirsten.kuesel@uni-jena.de.

Supplemental material for this article may be found at <http://dx.doi.org/10.1128/AEM.03844-15>.

Copyright © 2016, American Society for Microbiology. All Rights Reserved.

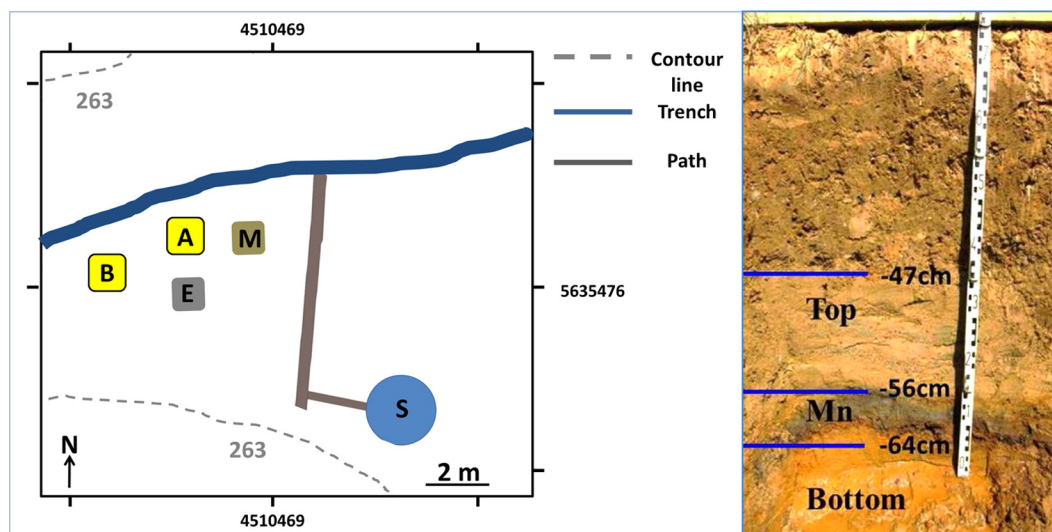


FIG 1 Schematic map of the sampling sites of the Mn deposit in the former uranium mining district Ronneburg, Germany (left), and the strata-like subsoil profile investigated (right). The strata-like secondary mineral deposit is unevenly distributed at this site and was subject of several studies. The map presents the sampling locations of the profile investigated in this study (A and B [a photo of the strata-like deposit was taken from location A]), which was also used for the isolation of low-pH Mn(II) oxidizers before by Akob et al. (5) (A), and adjacent sites used for studying metal retention by Burkhardt et al. (26) (E), mineral structure by Mayanna et al. (78) (M), and thermodynamic modeling by Schäffner et al. (1) (S).

These few studies provide the first glimpse into the bacteria involved in low-pH Mn oxidation and their relevant enzymes. However, questions remain regarding (i) whether the biological contribution is the main driver of low-pH Mn(II) oxidation because the rates of biological and chemical processes are both slow at acidic pH and largely dependent on the *in situ* environmental redox conditions (6, 23); (ii) whether there exists a special dominant Mn(II)-oxidizing microbial community adapted to low-pH conditions, compared to microbial communities in neutral to slightly alkaline environments; and (iii) whether Mn(II)-oxidizing microbial assemblages are spatially enriched with the secondary Mn minerals that may indicate a firm relationships between low-pH Mn(II) oxidizers and autochthonous Mn oxides.

In view of these questions, we investigated an epigenetic Mn deposit at a former uranium leaching site that is influenced by acidic (pH 4 to 5) and metalliferous groundwater with low levels of nutrients (24) and compared the microbial diversity of all three domains of life to those present in adjacent soil layers. To link phylogeny to function, we isolated bacterial and fungal key players involved in Mn(II) oxidation and compared the rates of Mn(II) depletion in soil microcosms studies amended with nutrients and/or biotic inhibitors. These results helped us to better understand biological Mn(II) oxidation in low-pH environments and advances our knowledge of potential strategies for the remediation of contaminated environments.

MATERIALS AND METHODS

Field site description. The sampling site (E 4510469, N 5635476 [Gauss-Krueger Potsdam coordinate system]) is at the former Gessenhalde leaching heap near Ronneburg (Fig. 1), which was one of the most important uranium mining areas of the former German Democratic Republic in the Cold War Era (24). During the 1970s to 1989, 6.8×10^6 m³ of low-grade uranium ore (Ordovician and Silurian black shale) was leached with acid mine drainage and sulfuric acid. Perpetual leakage caused tons of acids, metals, and radionuclides (such as Cd, Co, Cr, Fe, Mn, Ni, Pb, Zn, and U) to penetrate into the Pleistocene sediments and be introduced to ground-

water (6, 26–28). During the remediation that began at 1990, the leaching heap was removed and bulk of subjacent soil was excavated up to 10 m below the former land surface. Consequently, the deep quaternary sediment was exposed via this remediation process and covered later by only a 10- to 50-cm thickness of allochthonous soil materials (27). The groundwater table rose to –90 to –80 cm (1) after stopping the pumps, which were used to keep the water table low during mining.

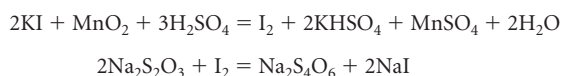
Elevated concentrations of dissolved and colloidal Mn and Fe enriched in the acidic and metals contaminated groundwater (26) was speculated as one of the plausible sources for metals that led to the development of a secondary mineral deposit below the heap through sediment capillary effects (1). The strata-like secondary mineral deposit in the Pleistocene sediments was approximately near the raised groundwater table after pumping ceased and is comprised now of three different mineralized layers (Fig. 1): (i) a silty sand layer consisting of Fe oxy/hydroxides with yellow-reddish color at the base of the strata (approximately –64 cm from the surface, referred to here as the “bottom layer”); (ii) a condensed, gray-to-black manganiferous sandy layer closely above the groundwater table (around –56 cm from the surface, referred to here as the “Mn layer”) with a thickness up to 13.5 cm but unevenly distributed within the former mining area; and (iii) a 0.1-m thick, yellow-to-gray oxyc layer with 75.5% sand and 24.3% silt (around –47 cm from the surface, referred to here as the “top layer”). The Mn layer is crumpled at the contact point with the bottom layer and has an average Eh of 650 ± 39 mV reflecting the favorable oxidizing conditions within the Mn layer (1). Metals such as Cd, Ni, Co, and Zn are conspicuously enriched and attenuated due to the strong scavenging of Mn oxides in the Mn layer (26).

Microbial activity and biomass are extremely low around and within the secondary mineral deposits (26). Bacterial 16S rRNA gene copy numbers were approximately 6.6×10^4 , 8.5×10^5 , and 6.1×10^5 per gram of soil for the top, Mn, and bottom layers, respectively (5), which is likely a millionth of the total bacterial cell numbers typically found in a gram of surface soil (28), corroborating the very low basal respiration rates of only $2 \text{ nmol g}^{-1} \text{ h}^{-1} \text{ CO}_2$ observed (26).

Sampling procedure. A randomized sampling strategy was applied (29). First, two 1-m-by-1-m-wide-by-0.4-m depth bulks of surface soil 2 m apart were excavated by spades. The first pit served as the main research site (referred to here as “site A”) (Fig. 1). Soils were sampled by a soil core

driller (PKH-100; MMM Tech Support, Germany) within the exposed 1-m-by-1-m area. Ten randomly drilled soil cores were immediately segmented with sterile spatulas based on visual inspection and depth, and pooled in sterile 50-ml Falcon tubes according to each layer. The tubes were cooled by liquid nitrogen or ice for DNA extraction and culture-dependent analysis, respectively. Groundwater was pumped manually using sterile 50-ml Omnifix syringes (B. Braun Medical, Inc., Germany) from the drilled holes of site A and maintained on ice during transportation. In the second pit (referred to here as "site B," Fig. 1), soil from the Mn layer was collected and pooled from eight randomly drilled soil cores and only used for comparison of microbial communities with samples from the Mn layer of site A, unless otherwise noted.

Physicochemical analysis. The pH of the soil was measured using the CaCl₂ method (30) and the water content by the thermogravimetric method (31). Total carbon and inorganic nitrogen were determined for all samples (dried at 105°C) using a LECO CNS-2000 Analyzer (Leco Corporation, St. Joseph, MI). Soil and groundwater for elemental analysis were prepared as previously described (26) and concentrations were measured using inductively coupled plasma mass spectrometry (XSeries II; Thermo Fisher Scientific) or inductively coupled plasma optical emission spectrometry (Spectroflame; Spectro). The total organic carbon (TOC) of the groundwater was analyzed using multi-N/C 2100S TOC analyzer (Analytik Jena AG, Germany). The average mass percentage of Mn oxide minerals was quantified by the Mn electron demand method based on the following chemical formulations (32):



Briefly, 0.25 g of air-dried soil sample was suspended in 20 ml of distilled deionized water (ddH₂O) in a calibrated 25-ml volumetric flask. A total of 2.5 ml of 3.61 M KI was added, followed by 1 ml of 18.4 M H₂SO₄. The suspension was stirred thoroughly for 12 h to completely reductively dissolve Mn oxides. The mixture was filtered through a 0.45- μm -pore size filter (Roth, Germany) and titrated with 0.1 M Na₂S₂O₃ until light yellow color occurred. Then, 1 ml of 0.5% starch solution was added, and the sample was titrated with standardized 0.1 M Na₂S₂O₃ until the blue color vanished. Mn(IV) oxide (99.99%; Aldrich) was used as a control. The mass percentage of Mn oxide minerals (normalized to MnO₂) was calculated as follows:

$$\text{Mn oxides \%} = \frac{0.5 \times C \times V \times M}{1,000 \times W} \times 100\%$$

where *C* is the concentration of Na₂S₂O₃ solution, which was 1 M in this experiment, *V* is the volume of Na₂S₂O₃ solution used for titration, *M* is the molecular weight of MnO₂, and *W* is the sample weight.

Electron probe X-ray microanalysis of the autochthonous Mn oxide minerals. Back-scattered electron images and chemical analyses of oxide minerals within the subsoil layers were performed on thin sections using a JEOL JXA 8230 electron microprobe. For this purpose, the samples were cleaned with distilled water, methanol, and liquid carbon dioxide, embedded in a low-viscosity epoxy resin, and subsequently ground, polished, and carbon coated. The microprobe was operated in wavelength-dispersive mode at an acceleration voltage of 15 kV and a beam current of 15 nA. Counting times on peak were 20 s for each element, except for Mg, Ca, and Cu with 30 s each. Background counting times were 50% of those on the peaks. The following X-ray lines and standards were used: Si K α , wollastonite; Al K α , corundum; Mg K α , periclase; Ba L α , barite; Ca K α , wollastonite; Ti K α , rutile; Fe K α , hematite; Mn K α , rhodonite; and Cu K α , chalcocopyrite. The raw data were corrected by applying the ϕ - ρ - z procedure (33).

DNA extraction, amplification, and microbial community profiling. Total DNA of the top, Mn, and bottom layers were extracted using a sodium dodecyl sulfate-based soil DNA extraction method (34). The quantity and quality of the extracted DNA was estimated using an ND-

1000 spectrophotometer (NanoDrop Technologies, Wilmington, DE). DNA samples with a concentration of at least 20 ng liter⁻¹ were sent to the Research and Testing Laboratory (Texas, USA) for tagged pyrosequencing. Archaeal and bacterial partial 16S rRNA genes were amplified by using the universal primer set 341F/958R and 28F/519R as previously described (35–37). Fungal ribosome small subunit-coding region (SSU) was sequenced using the primer set SSUFungiF and SSUFungiR as described previously (38). Sequences were treated as previously described (9) and analyzed using mothur version 1.34.4 (39).

Isolation and characterization of indigenous Mn(II) oxidizers. Mn(II)-oxidizing bacteria and fungi were isolated at a pH of 5.5 or 7.2 from a 10⁻¹ dilution in 0.7% NaCl of the Mn layer soil on modified PYG agar plates with (bacteria) or without (fungi) 0.05% cycloheximide. PYG agar contained per liter, 0.25 g of peptone, 0.25 g of yeast extract, 0.25 g of glucose, 20 g of agar, and 200 μM MnSO₄ (40), and the pH was buffered using 10 mM 2-(*N*-morpholino) ethanesulfonic acid (MES; Sigma) at pH 5.5 or HEPES (Sigma) at pH 7.2. The plates were incubated at 15°C in the dark. Single colonies were transferred five times by plate streaking. The leucocoberlin blue spot test was used to identify Mn(II) oxides as previously described (41).

Genomic DNA was extracted from a loopful cells of colonies on plates using the soil DNA extraction method described above (34). The DNA extract (1 μl) was PCR amplified using universal bacterial 16S rRNA gene primers 27F/1492R (42) and fungal internal transcribed spacer primers ITS1/ITS4 (43). Amplicons were sequenced at Macrogen, Inc. (Amsterdam, Netherlands) and assembled using Geneious Pro version 4.6.0 (44). Sequence similarity was determined using the BLAST algorithm against the NCBI GenBank database (45) and online identification service of EzTaxon database (46). Phylogenetic trees were constructed with the neighbor-joining algorithm using the MEGA 5.2 software package (47).

Mn(II) oxidation potential and mechanisms at acidic pH. Two microcosm experiments were designed to determine (i) the relative Mn(II) oxidation potential of the Mn layer versus the adjacent layers (microcosm I and II), (ii) the relative importance of the abiotic versus biotic mechanisms on Mn(II) oxidation (microcosm I), and (iii) the relative importance of fungi versus bacteria on Mn(II) oxidation (microcosm II). In microcosm I, the abiotic controls were conducted with HgCl₂ (25 mg liter⁻¹) to totally inhibit the activity of microorganisms (48), whereas in microcosm II, treatment with 0.05% cycloheximide served to inhibit fungal activity. Experiments were carried out in 100-ml Erlenmeyer flasks sealed with sterile cotton stoppers. Twelve-gram (wet weight) soil samples from the top, Mn, and bottom layers were suspended in 48 ml of either 1:4 sterilized ddH₂O-groundwater (microcosm I) or undiluted groundwater (microcosm II) to start with higher initial dissolved Mn(II) concentrations. The Mn(II) concentrations approximated 130 to 155 μM in microcosm I and 600 to 655 μM in microcosm II. No external Mn(II) was added into the microcosms. Glucose ($\geq 98\%$; Fluka) and NH₄Cl ($\geq 99.5\%$; Carl Roth, Germany) were added to some microcosms at final concentrations of 2 and 6 mM, respectively, as carbon and nitrogen sources to stimulate microbial activity. Microcosms were incubated at 15°C in the dark at 100 rpm on an orbital shaker. Three replicates of each treatment were destructively sampled periodically. The pH was measured at each of the sampling time points using a pH meter (pH-Electrode SenTix 41; WTW, Germany). To evaluate shifts in the bacterial community structure in the microcosms before and after biostimulation, total DNA from soils of all treatments were extracted and analyzed as described above at the terminal time point of Mn(II) linear depletion in microcosm II.

The Mn(II) depletion rate was measured on the filtered supernatant (0.2- μm -pore size nylon filter; Carl Roth, Germany) by the formaldoxime colorimetric method as previously described (49). To calculate the rate, a modified lumped zero-order reaction rate [$\mu\text{M Mn(II) h}^{-1} \text{ g soil}^{-1}$] was applied in both sets of the microcosms as previously described (50):

$$\frac{d[\text{Mn(II)}]}{dt} = ([\text{Mn(II)}]_0 - [\text{Mn(II)}]_t) \times V / (\Delta t \times M)$$

TABLE 1 Relative proportions of Mn/Fe/Ti oxide minerals in the different soil layers^a

Mineral	Formula	Relative proportions of different layers		
		Top	Mn	Bottom
Hematite	Fe ₂ O ₃	52	21	21
Goethite	Fe ³⁺ O(OH)	34	7	21
Anatase	TiO ₂	3	0	21
Ilmenite	Fe ²⁺ TiO ₃	7	10	32
Titano magnetite	Fe ²⁺ (Fe ³⁺ ,Ti) ₂ O ₄	3	3	4
Magnetite	Fe ²⁺ Fe ₂ ³⁺ O ₄	0	7	0
Romanechite	(Ba,H ₂ O) ₂ (Mn ⁴⁺ ,Mn ³⁺) ₅ O ₁₀	0	52	0
Total		100	100	100

^a The Mn/Fe/Ti oxides represented the total detectable oxides in the visual SEM field.

where t is the reaction time and Δt is the period during which the concentration of Mn(II) decreased linearly (hours), V is the volume of reactant (ml) in each flask, and M is the weight of inoculated soil (in grams). $Mn(II)_t$ and $Mn(II)_0$ are the final and initial concentrations, respectively, of Mn(II) in a time period during which the concentration of Mn(II) decreased linearly.

Four processes of Mn(II) depletion, the loss of Mn(II) from solution in the microcosms, were assumed as the major mechanisms: (i) abiotic oxidation, (ii) adsorption and precipitation, (iii) bacteria-related oxidation, and (iv) fungi-related oxidation. The total Mn(II) depletion rate was defined as a process, including all of the above mechanisms. The rates of Mn(II) depletion in the treatment with carbon and nitrogen amendment were used for calculating the total rate. We assumed 0.05% cycloheximide inhibited fungal activity. Therefore, the fungus-related contribution to Mn(II) oxidation was calculated based on the difference between the total rate and the rate of the treatment with the mixture of carbon, nitrogen, and 0.05% cycloheximide. Similarly, the bacterium-related contribution to Mn(II) oxidation was calculated based on the difference between the rate of the treatment with the mixture of carbon, nitrogen, and 0.05% cycloheximide and the rate of the treatment with only 0.05% cycloheximide.

Data analysis. The correlation between metal species with Mn oxide minerals was calculated by Pearson correlation coefficient using Graph-Pad Prism version 6.03. P values of <0.05 were considered statistically significant. All values are averages of at least three replicates. Microbial community statistical analysis were conducted in mothur (39), including rarefaction (sampling efficiency), and Chao, Shannon, and inverse Simpson indices (community richness and diversity). Relationships between physicochemical variables and microbial community structures were analyzed using canonical correspondence analysis (CCA) with Monte Carlo permutation test (Canoco 4.5) (51). Soil water content, pH, the concentration of N, Mn, Fe, As, Cu, Pb, Cr, U, and the mass percentage of MnO were chosen as the environmental variables in CCA because these factors are either vital for microbial activity or abundant in the Mn deposit and adjacent layers.

Nucleotide sequence accession numbers. The 16S rRNA gene sequences of MOB isolates determined in this study have been deposited in the European Nucleotide Archive (ENA) database under accession numbers LN852367 to LN852374. The sequence of the internal transcribed spacer region 1 (ITS1) of the fungal isolate obtained in this study was deposited in the ENA database under accession number LN876644. The pyrosequencing reads were deposited in the ENA database under study accession number PRJEB11431.

RESULTS

Soil physicochemical characteristics and autochthonous Mn oxides composition. The Mn layer had unique and distinct geochemical characteristics compared to the adjacent layers (see Table S1 in the supplemental material). This layer had the highest

total Mn content (7,550 $\mu\text{g/g}$), which was 6- to 7-fold greater than that of the bottom and top layers, and the highest percentage of Mn oxides (on average 31.45%) relative to only 0.57 and 1.57% in the top and bottom layers, respectively. Consequently, the Fe/Mn ratio was low with 4:1 in the Mn layer, followed 38:1 in the top layer and 33:1 in the bottom layer. Metals were enriched in all layers, whereas Cd and Ni showed affinity to the Mn layer. In general, all soils were acidic (pH 3.6 to 4.3), were low in total carbon and nitrogen, and showed gradual declines in water content from 18% (the bottom layer) to 14.6% (the top layer). The groundwater was characterized by pH 4.8, high concentrations of Mn (9,440 $\mu\text{g/liter}$) and metals such as Cu, Ni, Zn, and Cd (see Table S2 in the supplemental material), and high sulfate concentrations (824 mg/liter), whereas the nitrate level was <0.8 mg/liter.

Microanalytical investigations of polished thin sections from the different soil layers revealed various oxide minerals besides ubiquitous quartz, feldspar, and clay minerals. Mn oxides exclusively occurred in thin sections of the Mn layer in which they comprised $>50\%$ of all the oxides present (Table 1). The Mn oxides typically formed stellate crystalline aggregates of acicular crystals within the Mn layer. Commonly, they formed coatings on the surface of detrital grain particles with a Liesegang ring-like growth pattern (Fig. 2). Element mapping conducted by wavelength-dispersive X-ray spectrometry showed that Ba and Ca were in close spatial association with the Mn oxides. Quantitative mineralogical analyses revealed the Mn-mineral contains considerable amounts of Ba (9 to 12 wt%) and was determined as romanechite [ideal formula: $(\text{Ba},\text{H}_2\text{O})_2(\text{Mn}^{4+},\text{Mn}^{3+})_5\text{O}_{10}$] when aligned to the standard reference. Besides romanechite, ilmenite is the only Mn-bearing mineral phase among the present suite with ca. 3.8 wt% of MnO (see Table S3 in the supplemental material). Pearson correlation assay revealed that the poorly crystalline Mn oxides in the Mn layer displayed a positive correlation with Mg, Ca, and Cu ions but a statistically significant negative correlation with Fe ($P < 0.0001$) (see Table S4 in the supplemental material).

Microbial community profile in the Mn deposit and adjacent layers. Surprisingly, the greatest bacterial, archaeal, and fungal species richness (number of operational taxonomic units [OTU] on a 0.03 distance level) and diversity were observed in the Mn layers compared to the adjacent layers (see Fig. S1 and Table S5 in the supplemental material), suggesting the development of relatively different microbial communities.

Bacteria. Dendrograms generated by Jaccard index showed the bacterial community of the Mn layers in sites A and B shared more

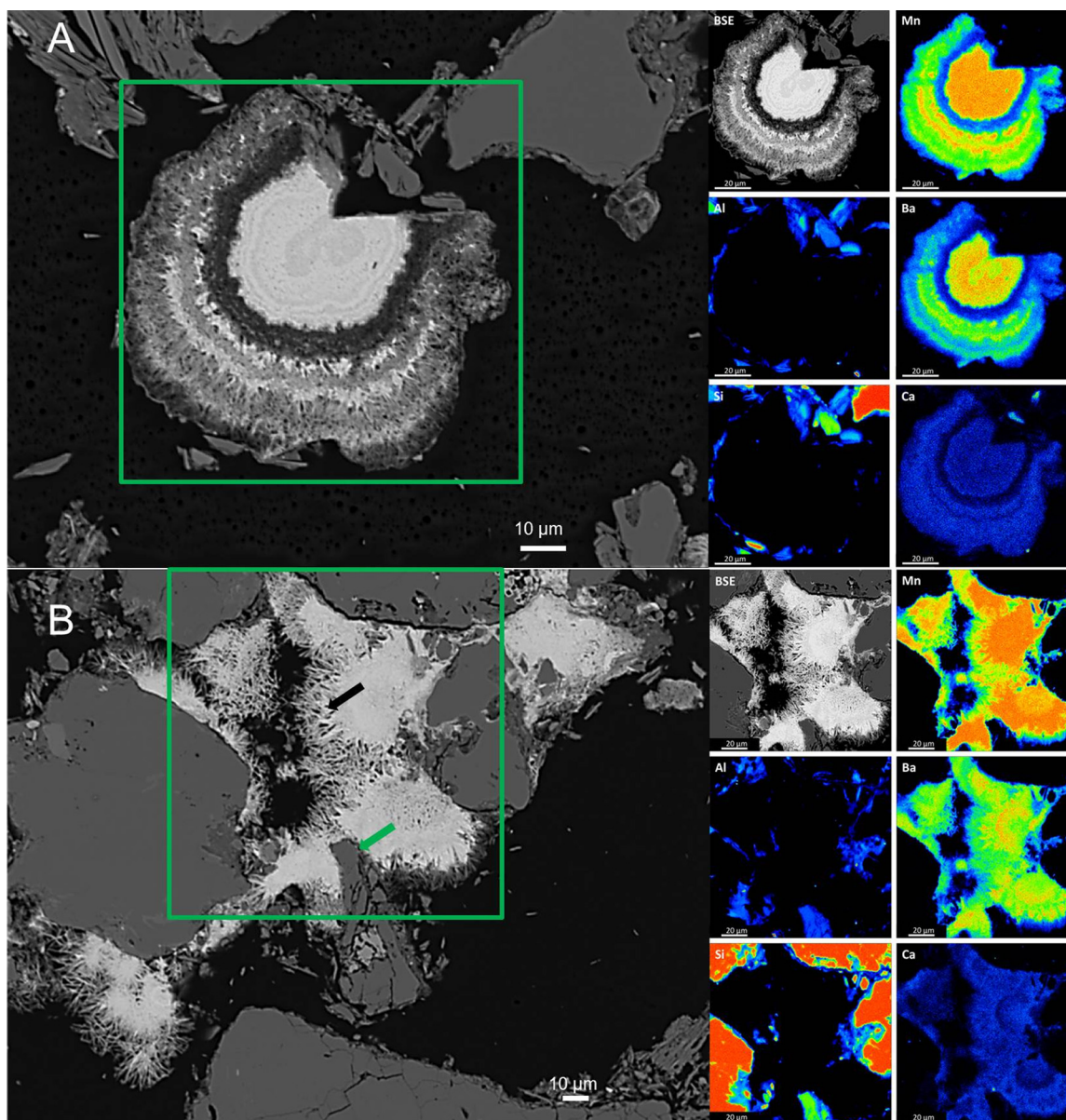


FIG 2 Electron microprobe image of two typical morphologies of the secondary Mn oxide minerals sampled from the Mn layer. (A) The stellate crystalline aggregates with a Liesegang ring-like growth pattern. (B) The acicular crystals (black arrow) coatings on the surface of detrital grain particles (green arrow). Element maps of the Mn oxides highlighted in the green box show enhanced intensities of Mn, Ba, and Ca (small panels to the right of panels A and B).

similarity whereas the communities in the top and bottom layers of site A clustered together (see Fig. S2 in the supplemental material). Approximately 165 different OTU were observed from 983 sequences of the Mn layer of site A. The species richness in the top and bottom layers were relatively lower with only 28 and 64 OTU detected from the normalized 983 reads. The Chao nonparametric richness estimator showed a similar pattern (see Table S5 in the supplemental material). In addition, Shannon and inverse Simpson indices showed greater microbial community diversity in the Mn layer of sites A and B. Examination of the bacterial taxonomic groups of sites A and B revealed a distinct structure in the Mn layer compared to that in the top and bottom layers. While *Proteobacteria* was the most abundant phylum recovered from the Mn and adjacent layers (Fig. 3), certain phyla were only detected in the Mn

layers, including *Elusimicrobia*, *Planctomycetes*, and *Chlorobi*. *Spirochaetae* solely appeared in the adjacent layers that no Mn oxides accumulated.

The presence and diversity of bacterial Mn(II) oxidizers within the Mn and adjacent layers were identified by 16S rRNA gene sequences closely related to known functional groups (Table 2). Tagged pyrosequencing revealed that the majority of known MOB occurred in the Mn layer compared to the top and bottom layers, where only four known MOB-related genera were detected. The potential MOB genera in the Mn layer included *Hyphomicrobium* (2.12%), *Rhizobium* (1.49%), *Arthrobacter* (0.96%), *Flavobacterium* (0.81%), *Gallionella* (0.59%), *Pseudomonas* (0.38%), *Leptothrix* (0.10%), *Rhodobacter* (0.10%), *Bacillus* (0.05%), *Streptomyces* (0.03%), *Roseobacter* (0.01%), and *Aurantimonas* (0.01%). In

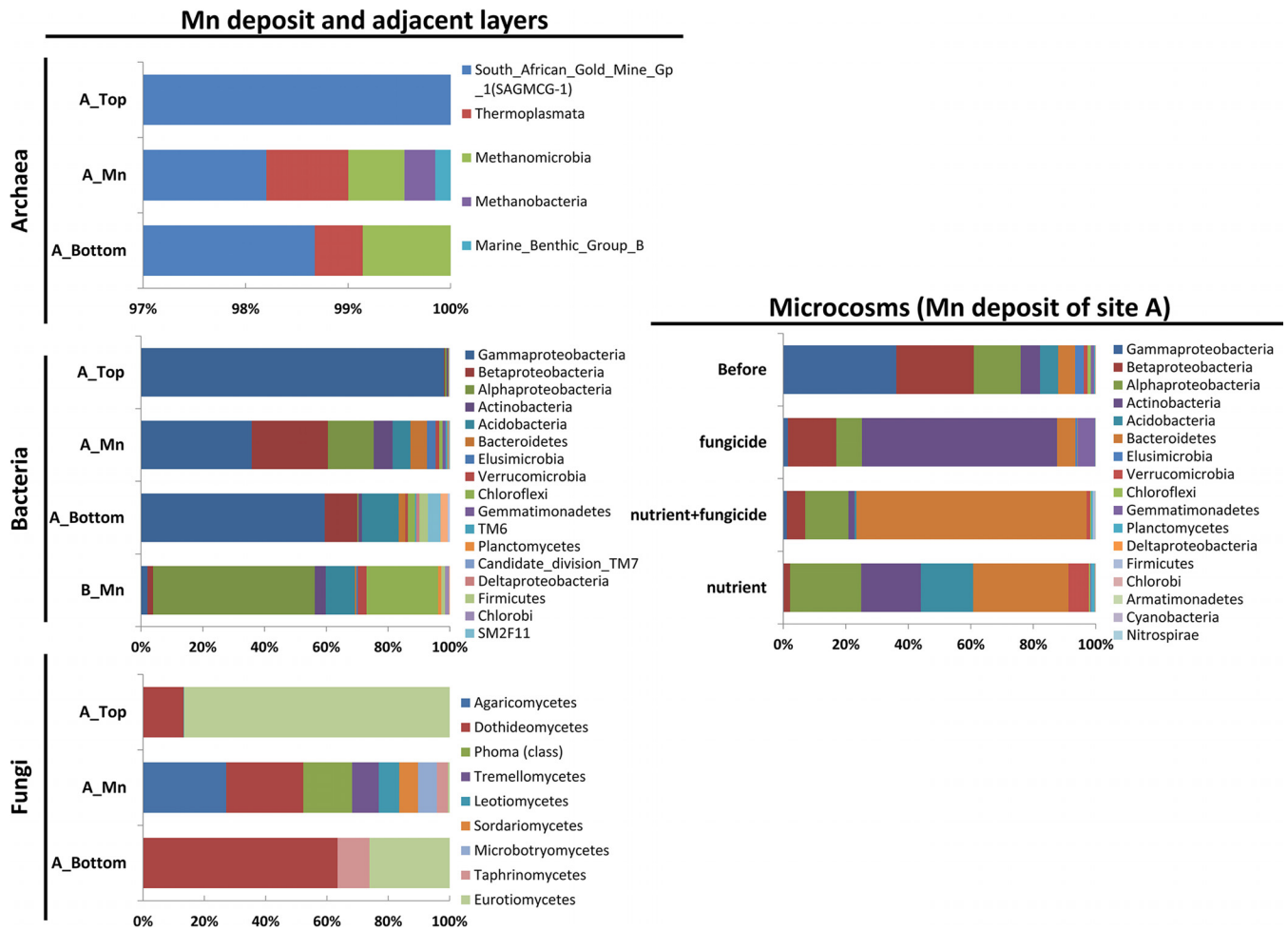


FIG 3 Relative abundance of microbial taxonomies in soil strata and microcosms. Microbial communities were characterized in the top, Mn, and bottom layers at site A and in the Mn layer of site B. Communities were analyzed in microcosm II from the Mn layer before and after biostimulation.

TABLE 2 Potential Mn(II)-oxidizing bacteria and fungi detected in soil strata using tagged pyrosequencing

Domain and genus	% total sequences ^a			Reference
	Top	Mn	Bottom	
Bacteria				
<i>Hyphomicrobium</i>	0.00	2.12	0.00	64
<i>Rhizobium</i>	0.00	1.49	0.00	87
<i>Arthrobacter</i>	0.00	0.96	0.00	88
<i>Flavobacterium</i>	0.00	0.81	1.94	10
<i>Gallionella</i>	0.00	0.59	0.00	89
<i>Pseudomonas</i>	9.22	0.38	11.62	14
<i>Leptothrix</i>	0.00	0.10	0.00	40
<i>Rhodobacter</i>	0.00	0.10	0.00	90
<i>Bacillus</i>	0.12	0.05	5.30	91
<i>Streptomyces</i>	0.00	0.03	0.00	21
<i>Roseobacter</i>	0.00	0.01	0.00	11
<i>Aurantimonas</i>	0.00	0.01	0.00	92
<i>Acinetobacter</i>	0.12	0.00	0.00	93
Fungi				
<i>Davidiella</i>	0.00	0.12	0.00	55
<i>Cladosporium</i>	0.00	13.02	20.49	53
<i>Alternaria</i>	1.70	0.00	0.00	18

The per-genus percentage of total sequences is presented.

contrast, *Pseudomonas*, which was often isolated as Mn(II) oxidizer from neutral to slight alkaline environments (14, 52–54), was the most abundant potential MOB in the top (9.22%) and bottom (11.62%) layers.

Archaea. The 5,631 high-quality 16S rRNA gene sequences recovered from the native archaeal communities were affiliated with two phyla *Euryarchaeota* and *Thaumarchaeota*. *Thaumarchaeota* were dominant in all layers (99% of total reads) and was represented by the most abundant class in the Mn layer being the South African Gold Mine Group 1 (SAGMG-1; 98%), coupled with an even distribution of *Thermoplasmata* and *Methanomicrobia* (Fig. 3). Marine Benthic Group B (MBG-B) and *Methanobacteria* were also present in the Mn layer. The top layer only contained organisms related to the SAGMG-1.

Fungi. Nine taxonomic groups (class level) recovered from the soil of the top, Mn, and bottom layers were dominated by sequences belonging to *Ascomycota* and *Basidiomycota*. Six taxonomic groups only appeared in the Mn layer, including *Agaricomycetes*, *Phoma* (class), *Tremellomycetes*, *Leotiomyces*, *Sordariomycetes*, and *Microbotryomycetes*. *Dothideomycetes* was prevalent in the bottom layer, whereas *Eurotiomycetes* was the most abundant class of fungi in the top layer. Retrieved fungal 18S

TABLE 3 Mn(II) oxidizers isolated from the Mn layer^a

Species	Representative isolate	Closest type strain (NCBI accession no., % similarity)	Isolation medium pH	Mn(II) oxidation at pH 5.5 ^b	Reported Mn(II) oxidation capacity (taxonomy)	Source or reference ^c
Bacteria						
<i>Arthrobacter humicola</i>	PclMES1	<i>Arthrobacter humicola</i> KV-653 (AB279890, 98.6)	5.5	+	+ (genus)	88
<i>Rhizobium soli</i>	PclMES2	<i>Rhizobium soli</i> DS-42 (EF363715, 99.69)	5.5	+	+ (genus)	87
<i>Aeromicrobium fastidiosum</i>	PclMES3	<i>Aeromicrobium fastidiosum</i> DSM10552 (Z78209, 99.18)	5.5	+	–	ND
<i>Aeromicrobium fastidiosum</i>	PclHEPES1	<i>Aeromicrobium fastidiosum</i> DSM10552 (Z78209, 99.26)	7.2	+	–	ND
<i>Pseudomonas graminis</i>	PclHEPES2	<i>Pseudomonas graminis</i> DSM11363 (Y11150, 99.57)	7.2	–	+ (genus)	14
<i>Hymenobacter metalli</i>	PclHEPES3	<i>Hymenobacter metalli</i> A2-91 (HM032898, 97.87)	7.2	–	–	ND
<i>Pseudomonas morrei</i>	PclHEPES4	<i>Pseudomonas moorei</i> RW10 (AM293566, 99.18)	7.2	–	+ (genus)	14
<i>Arthrobacter geryongensis</i>	PclHEPES5	<i>Arthrobacter geryongensis</i> DCY72 (JX141781, 99.11)	7.2	+	+ (genus)	88
Fungi						
<i>Cladosporium halotolerans</i>	PMES_TB3	<i>Cladosporium halotolerans</i> EXF-380 (DQ780368, 99.78)	5.5	+	+ (genus)	53

^a All isolates tolerated Mn(II) concentrations of >10 mM. Except for *Aeromicrobium* and *Hymenobacter*, all other isolates (genus) could be detected in the Mn deposit using pyrosequencing.

^b The “+” and “–” mean positive and negative results, respectively, for Mn(II) oxidation.

^c ND, no published report.

rRNA sequences closely related to known MOF groups revealed that *Cladosporium* and *Davidiella* (55) composed the majority of potential MOF in the Mn and bottom layers, whereas *Alternaria* (18) were found solely in the top layer (Table 2).

Isolation of indigenous low-pH Mn(II) oxidizers. We isolated eight MOB and one MOF from the 10^{−1} soil dilution of the Mn layer that tolerated Mn(II) concentrations of up to 10 mM (Table 3; see Fig. S3A to C in the supplemental material).

The MOB isolates belonged to five genera in the *Proteobacteria*, *Actinobacteria*, and *Bacteroidetes* phyla. Three recovered MOB—*Arthrobacter humicola* PclMES1, *Rhizobium soli* PclMES2, and *Aeromicrobium fastidiosum* PclMES3—oxidized Mn(II) at pH 5.5. From these, only *Arthrobacter* and *Rhizobium* were known as MOB at genus level (56, 57) (Table 3) and were relatively enriched in the Mn layer based on the pyrosequencing data. Members of the *Gammaproteobacteria* and *Bacteroidetes* were only isolated at pH 7.2, including *Pseudomonas graminis* PclHEPES2, *Pseudomonas fluorescens* PclHEPES4, and *Hymenobacter metalli* PclHEPES3 (see Fig. S3B in the supplemental material). *H. metalli* had not been shown previously to oxidize Mn(II) and was only capable of oxidation at pH 7.2 (Table 3). Members of the *Actinobacteria* phyla were the only ones isolated at both pH 5.5 and 7.2, and *Arthrobacter* and *Aeromicrobium* were the only two MOB genera that harbored species able to oxidize Mn(II) both under acidic and neutral conditions. *Arthrobacter humicola* PclMES1, *Pseudomonas graminis* PclHEPES2, *Pseudomonas fluorescens* PclHEPES4, and *Arthrobacter geryongensis* PclHEPES5 had sequences with 100% similarity with those detected in the pyrosequencing data set. At a similarity level of 96.0 to 100%, these isolates accounted for 0.36% of bacterial sequences in the Mn layer.

Only one Mn(II) oxidizing fungus, *Cladosporium halotolerans* PMES_TB3, was recovered from the Mn layer at pH 5.5. *Cladosporium* belongs to the order *Capnodiales* and is a genus of the phylum *Ascomycota* known to include Mn(II)-oxidizing fungi (58, 59).

Stimulated Mn(II) oxidation potentials and microbial communities. We compared Mn(II) oxidation potentials of top, Mn,

and bottom layer soils in microcosm incubation studies, which showed a significant difference in the rates of Mn(II) removal between the different soil strata, but only when nutrients (carbon and nitrogen) were added. In microcosm I, the Mn layer showed the highest Mn(II) depletion rate around 9.56 μM h^{−1} g soil^{−1} relative to 6.03 and 6.04 μM h^{−1} g soil^{−1} in the top and bottom layers, respectively. Without nutrient amendment no decrease in Mn(II) was observed despite the oxygenated conditions for over 138 h similar to the abiotic controls with HgCl₂ amendment (Fig. 4A to C). Pyrosequencing analyses revealed that the relative abundance of some bacterial phyla was higher in the Mn layer microcosm with carbon and nitrogen amendment after 84 h (Fig. 3) compared to the native soil, including *Alphaproteobacteria* (from 15 to 23%), *Actinobacteria* (from 6 to 19%), *Bacteroidetes* (from 5 to 31%), and *Acidobacteria* (from 6 to 17%). However, only one genus that is known to harbor MOB was enriched in this microcosm (*Arthrobacter* from 0.96 to 1.83%) (see Table S6 in the supplemental material).

In microcosm II, cycloheximide (0.05%) only partially inhibited Mn(II) depletion (Fig. 4D to F), suggesting that both bacteria and fungi are involved in Mn oxidation. The fungi-associated process dominated and mutually correlated with bacterium-associated process, accounting for 71 and 32% of the total Mn (II) depletion, respectively, in the Mn layer (Fig. 4E).

Biogeochemical coupling. CCA revealed that selected environmental variables in the Mn deposit and adjacent layers, including the availability of nitrogen and water, pH, Mn minerals, and metals, were associated with one another, as indicated by three clusters of vectors (Fig. 5). The distribution of total Mn and Mn oxides was closely related to soil pH, whereas iron, uranium, lead, and arsenic had a pronounced link with soil water content.

The influence of geological factors varied on the archaeal, bacterial, and fungal community. The eigenvalues, reflecting the significance of first canonical axis, were 0.007, 0.257, and 0.703, respectively. In the archaeal community, two classes, MBG-B and *Methanobacteria*, conspicuously associated with Mn and Mn oxides. In contrast, the distribution of the most abundant class,

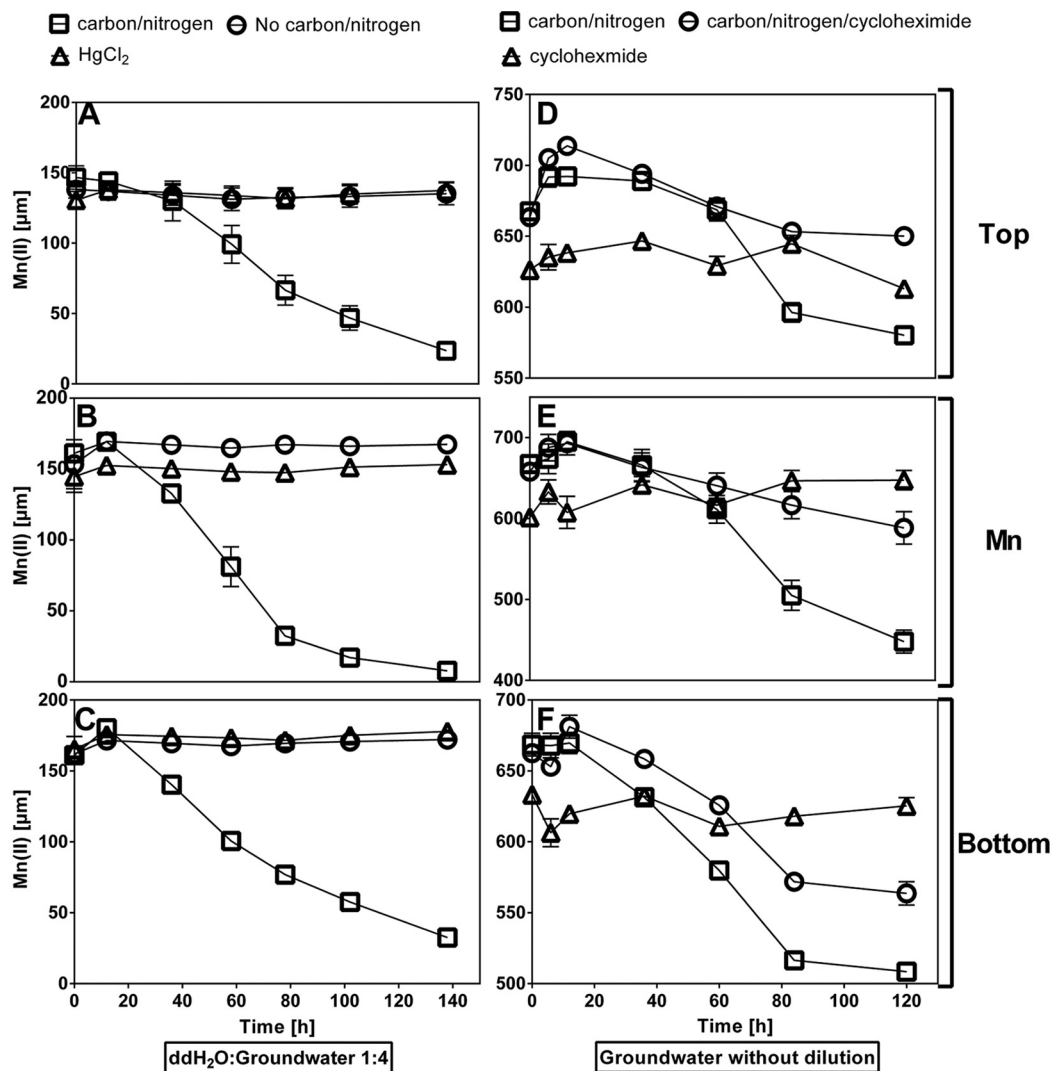


FIG 4 Mn(II) oxidation microcosm experiments. (A to C) Mn(II) depletion in microcosm I; (D to F) Mn(II) depletion in microcosm II. In the figures of microcosm II, triangle represents cycloheximide amendment with no carbon and nitrogen. The figures are vertically organized along the order of the top, Mn, and bottom layers. The error bar indicates the standard deviation.

SAGMG-1, showed no firm correlation with any selected variables. In the bacterial community, *Alphaproteobacteria*, *Betaproteobacteria*, *Actinobacteria*, and *Bacteroidetes* rather than *Firmicutes* firmly correlated with Mn oxides at acidic pH. A group of non-Mn(II)-oxidizing phyla [no model Mn(II)-oxidizing isolates reported], including *Planctomycetes*, *Gemmatimonadetes*, *Elusimicrobia*, *Chloroflexi*, *Verrucomicrobia*, and *Chlorobi*, displayed an exceptional affiliation with Mn and Mn oxides as well. The fungal distribution was considerably constrained by the soil pH, total Mn, and Mn oxides. Approximately 67% of the taxonomic groups (order) correlated with Mn and Mn oxides.

DISCUSSION

The study presented here shows cumulative evidence that low-pH-adapted microorganisms are the main force for Mn(II) oxidation in the acidic Mn deposit. Many bacteria and fungi known for Mn(II) oxidation were present in the Mn deposit, and their activity might have affected other geochemical processes (e.g.,

metal attenuation and nitrogen and carbon cycling). Interdependently, biogenic Mn oxides appeared to serve as a suitable microenvironment and may shelter and benefit a niche-specific microbial community in the acidic, oligotrophic, and metalliferous ecosystems.

The Mn layer harbored an increased diversity of adapted microorganisms. The Mn deposit harbored a more diverse microbial community that was structurally different from the top and bottom layers. Although *Proteobacteria* was the dominant bacterial phylum in the Mn deposit and the adjacent layers, the majority of known MOB were only present in the Mn layer according to the tagged pyrosequencing data. *Hyphomicrobium* and *Rhizobium* were the top two abundant MOB genera that were only present in the Mn layer. Intriguingly, these two genera share a lot of similarities. First, *Hyphomicrobium* and *Rhizobium* are both prosthecate bacteria that possess cellular appendages which are extensions of the cellular membrane, allowing a greater surface area to take up nutrients and trace metals in oligotrophic habitats (60, 61). Fur-

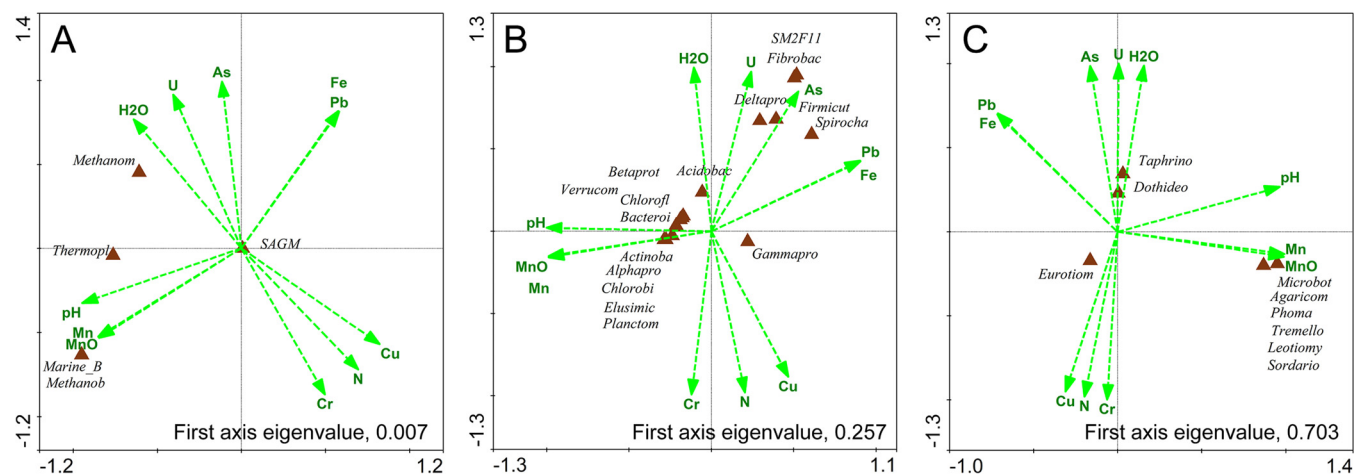


FIG 5 Canonical correspondence analysis (CCA) of indigenous microbial communities and selected environmental variables. Microbial taxonomic groups are presented as triangles. Panels A, B, and C show the results of archaeal, bacterial, and fungal communities, respectively. Names of all microbial groups (taxa) are truncated to only the first eight characters due to software limitations.

thermore, *Hyphomicrobium* and *Rhizobium* have been both found enriched in oligotrophic cave ferromanganese deposits (62, 63). Both are capable of denitrification and nitrogen fixation (64, 65), suggesting that Mn(II)-oxidizing bacteria might play an essential role for coupling nitrogen biogeochemical cycling and manganese oxidation in oligotrophic terrestrial niches. These bacteria have been found also in a neutral to slightly alkaline cave (63), implying *Hyphomicrobium* and *Rhizobium* as Mn(II) oxidizers tolerant a wide pH range.

Because genomic information and phylogenetic relationships do not provide clear evidence, we also tried to obtain isolates to yield further insights into novel hitherto unknown MOB and MOF present in the Mn deposit and their ecophysiology. Our new MOB isolate *Hymenobacter metalli* PclHEPES3 was closely related to a species isolated from a uranium mine (Urgeiriça, Central Portugal) which was shown to tolerate metal-rich circumstances (66), implying that PclHEPES3 might play a role in the interaction between metals and biogenic Mn oxides at acidic pH. We also found two MOB isolates from the genera *Arthrobacter* and *Aeromicrobium* that oxidized Mn(II) both at pH 5.5 and pH 7.2, indicating that pH might not affect the Mn(II) oxidizing pathway used by these MOB or they apply a binary strategy on Mn(II) oxidation to comply the shifting pH as seen for *Mesorhizobium australicum* T-G1 (6). Intriguingly, *Pseudomonas*, represented by isolates PclHEPES2 and PclHEPES4, only oxidized Mn(II) at pH 7.2 even though they were isolated from an acidic environment, implying the Mn(II) oxidation capacity of certain indigenous MOB is pH related. This was further verified by our finding that *Rhizobium soli* strain PclMES2 only oxidized Mn(II) at pH 5.5 but not pH 7.2, similar with previous findings of *Duganella* sp. strain AB_14 and *Albidiferax ferrireducens* strain TB-2, which were also isolated from a Mn subsoil layer in the same former uranium mining area (5).

Several archaeal classes, including MBG-B, *Methanobacteria*, *Methanomicrobia*, *Thermoplasmata*, and SAGMCG-1, were observed in the Mn layer. No member of the MBG-B has so far been isolated in pure culture, and thus their physiology and metabolism remain unknown. However, correlation analysis between 16S rRNA gene abundance and geochemical parameters of sediments

in the Arctic ocean suggested that they were involved in organic carbon as well as in manganese cycling (67), which explained why the MBG-B was only detected in the Mn layer. The SAGMCG-1 was the dominant group of the archaeal community in the acidic Mn deposit and also prevailed in the adjacent environments. The archaea of SAGMCG-1 were initially detected from mines which harbor unique environments, including metalliferous groundwater ecosystems, pores between mineral grains or inside rocks, and acidic mine drainage (68). To date, there exists only one cultured representative of the SAGMCG-1 archaea, *Nitrosotalea* sp., which is an acidic ammonia oxidizer (69). Their tolerance to acidic and metalliferous conditions habitats would explain their prevalence in the acidic mining site.

Similar to the native bacterial and archaeal communities, the greatest fungal species richness and diversity were observed in the Mn layer, further implying a firm relationship between indigenous fungal community and biogenic Mn oxides. Known as Mn(II) oxidizers (8, 9, 70, 71), *Agaricomycetes*, *Sordariomycetes*, and *Phoma* (class) were only detected in the Mn layer. Similarly, *Tremellomycetes* and *Leotiomyces*, not yet known for Mn oxidation, were only present in the Mn layer, but they have been found dominant in Mn-rich environments (9). Their genomes both plausibly harbor the Mn oxidation I pathway (<http://fungicyc.broadinstitute.org/>), indicating their potential capacity for Mn(II) oxidation. *Cladosporium halotolerans*, represented by isolate PMES_TB3, was the only known MOF (58, 59) that was isolated from the Mn deposit. *C. halotolerans* tolerates hypersaline environments (58), but a potential correlation between resistance and Mn(II) oxidation would necessitate further investigation. Although the exclusive presence of many MOB and MOF in the Mn deposit suggests microbial participation in Mn oxidation at low pH, we could not demonstrate microbial activity using microcosms without further nutrient amendment. Nonetheless, we showed that native microorganisms initiate the reaction when carbon and nitrogen were added despite the fact that low pH may negatively affect Mn(II) oxidation and hamper the reaction rate (72). Physical adsorption of Mn(II) on Mn precipitates in the microcosms should be ruled out because the ratio of the biotic contribution on Mn(II) oxidation in the microcosms of Mn layer

was slightly higher than the ratio of total Mn(II) depletion. Furthermore, the MOB activated under these nutrient conditions, like *Arthrobacter*, might not be the key players in such an oligotrophic habitat.

Biogenic Mn oxides and their influence on the acidic, oligotrophic, and metalliferous ecosystems. Several findings point to a biological origin of the Mn oxides found in the deposit of the acidic uranium mining area. Mn oxides produced by microorganisms often differ in morphology, composition, and crystal structure from those formed by geologic mechanisms; they often consist of stacked hexagonal sheets of MnO₆ octahedra with extremely small particle sizes and numerous structural defects (73). The prominently occurring romanechite-like Mn oxides are tunnel structure oxides constructed by double and triple chains of edge-sharing MnO₆ octahedra (4), which are often found as dendrites and coatings on the rock surface. Previous works have also revealed that romanechite is likely to be one of the biogenic Mn oxides in nature (73–77). Larger scale field studies revealed birnessite and todorokite as the main species of the autochthonous Mn minerals in the Mn deposit at this site (1, 78), and these minerals are often biogenic origin (73). Birnessite is a phyllo-manganate with a ~10-Å d-spacing and intends to be transferred to todorokite, which has the same structure as romanechite (79–81). In addition, we found a pronounced correlation between the autochthonous Mn oxide and Ca²⁺ which normally act as cofactors in biological systems, implying a firm association of the native biota and the Mn oxide minerals (82).

Furthermore, the fine Liesegang ring-like structure of the autochthonous Mn oxides might suggest a progressive mineralization process over the years, concomitantly with the dynamic balance of Mn(II) concentration found in the groundwater-affected porewater of the subsoil of the former uranium leaching heap (1). A slow mineralization process was explained by a slow activity of microorganisms in this oligotrophic ecosystem which are present in very low abundance compared to surface soils (5) and their low basal respiration rates (26).

CCA showed that in addition to *Alphaproteobacteria* and *Betaproteobacteria*, a substantial portion of rare bacterial OTU, including *Planctomycetes*, *Gemmatimonadetes*, and *Synergistetes*, which were not known as Mn(II) oxidizers before, strongly associated with Mn oxides, indicating that the Mn oxides might fundamentally sustain the indigenous bacterial community. Corroboratively, He et al. reported that *Planctomycetes*, *Gemmatimonadetes*, and *Nitrospirae* occurred in acidic soil Mn nodules as well (83). MBG-B and *Methanobacteria* were also apparently associated with Mn and Mn oxides. A previous study reported that MBG-B and *Methanobacteria* showed significant covariation with Mn ($P < 0.0000$) (70) and that the oxidation of methane is Mn dependent in marine ecosystems (84), indicating a direct or indirect link to manganese cycling.

The indigenous fungal community was highly constrained by geogenic variables, in particular Mn oxides. Vaughan et al. recently reported that fungal communities in oligotrophic environments were constrained more by spatiotemporal parameters rather than nutrients (85). Therefore, the aforementioned observations might reflect geogenic variables based control on fungal ecofunction and diversity.

We postulate here that because of the physicochemical characteristics of mineral structure (e.g., low crystallinity, large amorphous area, and high negative surface charge) (86), Mn oxides

may form microenvironments to shelter a niche-specific microbial community. While the Mn mineral deposit was oligotrophic, diverse nitrogen cycling related Mn(II)-oxidizing microorganisms occurred indigenously, suggesting the redox of Mn firmly coupled with the nitrogen cycle at acidic pH. Intriguingly, CCA analysis showed inorganic nitrogen firmly associated with metals such as copper and chromium in the Mn deposit and adjacent layers, indicating a potential correlation between nitrogen cycling and metal attenuation. Therefore, our results demonstrated that Mn(II)-oxidizing microorganisms, together with biogenic Mn oxides, might be vital for sustaining microbial biota in acidic, oligotrophic, and metalliferous subsoil ecosystems.

ACKNOWLEDGMENTS

We thank Susan Trumbore (MPI for Biogeochemistry Jena) for help with soil carbon and nitrogen analysis. We are grateful to Kate Campbell and Kevin J. Breen for their valuable comments.

We thank the Deutsche Forschungsgemeinschaft (DFG GRK 1257) for funding.

Any use of trade, product, or firm names is for descriptive purposes only and does not imply endorsement by the U.S. Government. The authors declare no competing financial interest.

FUNDING INFORMATION

This work, including the efforts of Tsing Bohu and Kirsten Küsel, was funded by Deutsche Forschungsgemeinschaft (DFG) (DFG GRK 1257).

REFERENCES

- Schäffner F, Merten D, Pollok K, Wagner S, Knoblauch S, Langenhorst F, Büchel G. 2015. Fast formation of supergene Mn oxides/hydroxides under acidic conditions in the oxic/anoxic transition zone of a shallow aquifer. *Environ Sci Pollut Res* 22:19362–19375. <http://dx.doi.org/10.1007/s11356-015-4404-z>.
- Komárek M, Vaněk A, Ettler V. 2013. Chemical stabilization of metals and arsenic in contaminated soils using oxides: a review. *Environ Pollut* 172:9–22. <http://dx.doi.org/10.1016/j.envpol.2012.07.045>.
- Nordstrom DK. 2000. Advances in the hydrogeochemistry and microbiology of acid mine waters. *Int Geol Rev* 42:499–515. <http://dx.doi.org/10.1080/00206810009465095>.
- Post JE. 1999. Manganese oxide minerals: Crystal structures and economic and environmental significance. *Proc Natl Acad Sci U S A* 96:3447–3454. <http://dx.doi.org/10.1073/pnas.96.7.3447>.
- Akob DM, Bohu T, Beyer A, Schäffner F, Händel M, Johnson CA, Merten D, Büchel G, Totsche KU, Küsel K. 2014. Identification of Mn(II)-oxidizing bacteria from a low-pH contaminated former uranium mine. *Appl Environ Microbiol* 80:5086–5097. <http://dx.doi.org/10.1128/AEM.01296-14>.
- Bohu T, Santelli CM, Akob DM, Neu TR, Ciobota V, Rösch P, Popp J, Nietzsche S, Küsel K. 2015. Characterization of pH dependent Mn(II) oxidation strategies and formation of a bixbyite-like phase by *Mesorhizobium australicum* T-G1. *Front Microbiol* 6:734. <http://dx.doi.org/10.3389/fmicb.2015.00734>.
- Tebo BM, Johnson HA, McCarthy JK, Templeton AS. 2005. Geomicrobiology of manganese(II) oxidation. *Trends Microbiol* 13:421–428. <http://dx.doi.org/10.1016/j.tim.2005.07.009>.
- Santelli CM, Pfister DH, Lazarus D, Sun L, Burgos WD, Hansel CM. 2010. Promotion of Mn(II) oxidation and remediation of coal mine drainage in passive treatment systems by diverse fungal and bacterial communities. *Appl Environ Microbiol* 76:4871–4875. <http://dx.doi.org/10.1128/AEM.03029-09>.
- Chaput DL, Hansel CM, Burgos WD, Santelli CM. 2015. Profiling microbial communities in manganese remediation systems treating coal mine drainage. *Appl Environ Microbiol* 81:2189–2198. <http://dx.doi.org/10.1128/AEM.03643-14>.
- Carmichael MJ, Carmichael SK, Santelli CM, Strom A, Bräuer SL. 2013. Mn(II)-oxidizing bacteria are abundant and environmentally relevant members of ferromanganese deposits in caves of the upper Tennessee river

- basin. *Geomicrobiol J* 30:779–800. <http://dx.doi.org/10.1080/01490451.2013.769651>.
11. Hansel CM, Francis CA. 2006. Coupled photochemical and enzymatic Mn(II) oxidation pathways of a planktonic *Roseobacter*-like bacterium. *Appl Environ Microbiol* 72:3543–3549. <http://dx.doi.org/10.1128/AEM.72.5.3543-3549.2006>.
 12. Bargar JR, Tebo BM, Bergmann U, Webb SM, Glatzel P, Chiu VQ, Villalobos M. 2005. Biotic and abiotic products of Mn(II) oxidation by spores of the marine *Bacillus* sp. strain SG-1. *Am Mineral* 90:143–154. <http://dx.doi.org/10.2138/am.2005.1557>.
 13. Corstjens PLAM, de Vrind JPM, Goosen T, de Vrind-de Jong EW. 1997. Identification and molecular analysis of the *Leptothrix discophora* SS-1 *mofA* gene, a gene putatively encoding a manganese-oxidizing protein with copper domains. *Geomicrobiol J* 14:91–108. <http://dx.doi.org/10.1080/01490459709378037>.
 14. Brouwers GJ, de Vrind JP, Corstjens PL, Cornelis P, Baysse C, de Vrind-de Jong EW. 1999. *cumA*, a gene encoding a multicopper oxidase, is involved in Mn²⁺ oxidation in *Pseudomonas putida* GB-1. *Appl Environ Microbiol* 65:1762–1768.
 15. Anderson CR, Johnson HA, Caputo N, Davis RE, Torpey JW, Tebo BM. 2009. Mn(II) oxidation is catalyzed by heme peroxidases in “*Aurantimonas manganoxydans*” strain SI85-9A1 and *Erythrobacter* sp. strain SD-21. *Appl Environ Microbiol* 75:4130–4138. <http://dx.doi.org/10.1128/AEM.02890-08>.
 16. Könneke M, Bernhard AE, de la Torre JR, Walker CB, Waterbury JB, Stahl DA. 2005. Isolation of an autotrophic ammonia-oxidizing marine archaeon. *Nature* 437:543–546. <http://dx.doi.org/10.1038/nature03911>.
 17. Stein LY, La Duc MT, Grundl TJ, Nealson KH. 2001. Bacterial and archaeal populations associated with freshwater ferromanganese micronodules and sediments. *Environ Microbiol* 3:10–18. <http://dx.doi.org/10.1046/j.1462-2920.2001.00154.x>.
 18. Hansel CM, Zeiner CA, Santelli CM, Webb SM. 2012. Mn(II) oxidation by an ascomycete fungus is linked to superoxide production during asexual reproduction. *Proc Natl Acad Sci U S A* 109:12621–12625. <http://dx.doi.org/10.1073/pnas.1203885109>.
 19. Nealson KH. 2006. The manganese-oxidizing bacteria, p 222–231. *In* Dworkin M, Falkow S, Rosenberg E, Schleifer KH, Stackebrandt E (ed), *The prokaryotes*. Springer, New York, NY.
 20. Luther GW, III. 2010. The role of one- and two-electron transfer reactions in forming thermodynamically unstable intermediates as barriers in multi-electron redox reactions. *Aquat Geochem* 16:395–420. <http://dx.doi.org/10.1007/s10498-009-9082-3>.
 21. Bromfield SM. 1979. Manganous ion oxidation at pH values below 5.0 by cell-free substances from *Streptomyces* sp. cultures. *Soil Biol Biochem* 11:115–118. [http://dx.doi.org/10.1016/0038-0717\(79\)90086-5](http://dx.doi.org/10.1016/0038-0717(79)90086-5).
 22. Ivarson KC, Heringa PK. 1972. Oxidation of manganese by microorganisms in manganese deposits of Newfoundland soil. *Can J Soil Sci* 52:401–416. <http://dx.doi.org/10.4141/cjss72-052>.
 23. Stumm W, Morgan JJ. 2012. *Aquatic chemistry: chemical equilibria and rates in natural waters*. John Wiley & Sons, New York, NY.
 24. Gatzweiler R, Jahn S, Neubert G, Paul M. 2001. Cover design for radioactive and AMD-producing mine waste in the Ronneburg area, Eastern Thuringia. *Waste Manag* 21:175–184. [http://dx.doi.org/10.1016/S0956-053X\(00\)00060-X](http://dx.doi.org/10.1016/S0956-053X(00)00060-X).
 25. Grawunder A, Lonschinski M, Merten D, Büchel G. 2015. Rare earth elements as a tool for studying the formation of cemented layers in an area affected by acid mine drainage. *Appl Geochem* 54:100–110. <http://dx.doi.org/10.1016/j.apgeochem.2015.01.006>.
 26. Burkhardt EM, Meißner S, Merten D, Büchel G, Küsel K. 2009. Heavy metal retention and microbial activities in geochemical barriers formed in glacial sediments subjacent to a former uranium mining leaching heap. *Chem Erde Geochem* 69:21–34. <http://dx.doi.org/10.1016/j.chemer.2008.12.003>.
 27. Schäffner F. 2013. Natural attenuation of heavy metals in near-surface supergene Mn deposits occurring heap, Ronneburg, Germany. PhD thesis. Friedrich-Schiller University Jena, Jena, Germany.
 28. Taylor JP, Wilson B, Mills MS, Burns RG. 2002. Comparison of microbial numbers and enzymatic activities in surface soils and subsoils using various techniques. *Soil Biol Biochem* 34:387–401. [http://dx.doi.org/10.1016/S0038-0717\(01\)00199-7](http://dx.doi.org/10.1016/S0038-0717(01)00199-7).
 29. Tan KH. 2005. *Soil sampling, preparation, and analysis*, 2nd ed. CRC Press, Boca Raton, FL.
 30. Schofield RK, Taylor AW. 1955. The measurement of soil pH. *Soil Sci Soc Am J* 19:164. <http://dx.doi.org/10.2136/sssaj1955.03615995001900020013x>.
 31. Smith KA. 2000. *Soil and environmental analysis: physical methods*, revised, and expanded. CRC Press, Boca Raton, FL.
 32. Bartlett RJ. 1988. Manganese redox reactions and organic interactions in soils, p 59–73. *In* Graham RD, Hannam RJ, Uren NC (ed), *Manganese in soils and plants*. Springer, Amsterdam, Netherlands.
 33. Armstrong JT. 1988. Quantitative analysis of silicate and oxide minerals: comparison of Monte Carlo, ZAF and ϕ - ρ - z procedures, p 239–246. *In* Newbury DE (ed), *Microbeam analysis*. San Francisco Press, San Francisco, CA.
 34. Zhou J, Bruns MA, Tiedje JM. 1996. DNA recovery from soils of diverse composition. *Appl Environ Microbiol* 62:316–322.
 35. Suchodolski JS, Dowd SE, Westermark E, Steiner JM, Wolcott RD, Spillmann T, Harmoinen JA. 2009. The effect of the macrolide antibiotic tylosin on microbial diversity in the canine small intestine as demonstrated by massive parallel 16S rRNA gene sequencing. *BMC Microbiol* 9:210. <http://dx.doi.org/10.1186/1471-2180-9-210>.
 36. Duc MTL, Vaishampayan P, Nilsson HR, Torok T, Venkateswaran K. 2012. Pyrosequencing-derived bacterial, archaeal, and fungal diversity of spacecraft hardware destined for mars. *Appl Environ Microbiol* 78:5912–5922. <http://dx.doi.org/10.1128/AEM.01435-12>.
 37. Dowd SE, Sun Y, Secor PR, Rhoads DD, Wolcott BM, James GA, Wolcott RD. 2008. Survey of bacterial diversity in chronic wounds using Pyrosequencing, DGGE, and full ribosome shotgun sequencing. *BMC Microbiol* 8:43. <http://dx.doi.org/10.1186/1471-2180-8-43>.
 38. Dowd SE, Delton Hanson J, Rees E, Wolcott RD, Zischau AM, Sun Y, White J, Smith DM, Kennedy J, Jones CE. 2011. Survey of fungi and yeast in polymicrobial infections in chronic wounds. *J Wound Care* 20:40–47. <http://dx.doi.org/10.12968/jowc.2011.20.1.40>.
 39. Schloss PD, Westcott SL, Ryabin T, Hall JR, Hartmann M, Hollister EB, Lesniewski RA, Oakley BB, Parks DH, Robinson CJ, Sahl JW, Stres B, Thallinger GG, Horn DJV, Weber CF. 2009. Introducing mothur: open-source, platform-independent, community-supported software for describing and comparing microbial communities. *Appl Environ Microbiol* 75:7537–7541. <http://dx.doi.org/10.1128/AEM.01541-09>.
 40. Emerson D, Ghiorse WC. 1992. Isolation, cultural maintenance, and taxonomy of a sheath-forming strain of *Leptothrix discophora* and characterization of manganese-oxidizing activity associated with the sheath. *Appl Environ Microbiol* 58:4001–4010.
 41. Krumbein WE, Altmann HJ. 1973. A new method for the detection and enumeration of manganese oxidizing and reducing microorganisms. *Helgol Wiss Meeresunters* 25:347–356. <http://dx.doi.org/10.1007/BF01611203>.
 42. Lane DJ. 1991. 16S/23S rRNA sequencing, p 115–175. *In* Stackebrandt E, Goodfellow M (ed), *Nucleic acid techniques in bacterial systematics*. Wiley, London, United Kingdom.
 43. White TJ, Bruns T, Lee S, Taylor J. 1990. Amplification and direct sequencing of fungal ribosomal RNA genes for phylogenetics, p 315–322. *In* Innis MA, Gelfand DH, Sninsky JJ, White TJ (ed), *PCR protocols: a guide to methods and applications*. Academic Press, Inc, New York, NY.
 44. Drummond A, Ashton B, Buxton S, Cheung M, Cooper A, Duran C. 2009. Geneious version (v4.6.0). Biomatters, Ltd, Auckland, New Zealand.
 45. Altschul SF, Gish W, Miller W, Myers EW, Lipman DJ. 1990. Basic local alignment search tool. *J Mol Biol* 215:403–410. [http://dx.doi.org/10.1016/S0022-2836\(05\)80360-2](http://dx.doi.org/10.1016/S0022-2836(05)80360-2).
 46. Kim OS, Cho YJ, Lee K, Yoon SH, Kim M, Na H, Park SC, Jeon YS, Lee JH, Yi H, Won S, Chun J. 2012. Introducing EzTaxon-e: a prokaryotic 16S rRNA gene sequence database with phylotypes that represent uncultured species. *Int J Syst Evol Microbiol* 62:716–721. <http://dx.doi.org/10.1099/ijs.0.038075-0>.
 47. Tamura K, Peterson D, Peterson N, Stecher G, Nei M, Kumar S. 2011. MEGA5: molecular evolutionary genetics analysis using maximum likelihood, evolutionary distance, and maximum parsimony methods. *Mol Biol Evol* 28:2731–2739. <http://dx.doi.org/10.1093/molbev/msr121>.
 48. Vancheswaran S, Hyman MR, Semprini L. 1999. Anaerobic biotransformation of trichlorofluoroethene in groundwater microcosms. *Environ Sci Technol* 33:2040–2045. <http://dx.doi.org/10.1021/es9811952>.
 49. Emerson S, Kalthorn S, Jacobs L, Tebo BM, Nealson KH, Rosson RA. 1982. Environmental oxidation rate of manganese(II): bacterial catalysis. *Geochim Cosmochim Acta* 46:1073–1079. [http://dx.doi.org/10.1016/0016-7037\(82\)90060-6](http://dx.doi.org/10.1016/0016-7037(82)90060-6).
 50. Luan F, Santelli CM, Hansel CM, Burgos WD. 2012. Defining manga-

- nese(II) removal processes in passive coal mine drainage treatment systems through laboratory incubation experiments. *Appl Geochem* 27: 1567–1578. <http://dx.doi.org/10.1016/j.apgeochem.2012.03.010>.
51. ter Braak CJF. 1986. Canonical correspondence analysis: a new eigenvector technique for multivariate direct gradient analysis. *Ecology* 67:1167–1179. <http://dx.doi.org/10.2307/1938672>.
 52. Geszvain K, Yamaguchi A, Maybee J, Tebo BM. 2011. Mn(II) oxidation in *Pseudomonas putida* GB-1 is influenced by flagella synthesis and surface substrate. *Arch Microbiol* 193:605–614. <http://dx.doi.org/10.1007/s00203-011-0702-0>.
 53. Geszvain K, McCarthy JK, Tebo BM. 2013. Elimination of manganese(II,III) oxidation in *Pseudomonas putida* GB-1 by a double knockout of two putative multicopper oxidase genes. *Appl Environ Microbiol* 79:357–366. <http://dx.doi.org/10.1128/AEM.11850-12>.
 54. Okazaki M, Sugita T, Shimizu M, Ohode Y, Iwamoto K, de Vrind-de Jong EW, de Vrind JP, Corstjens PL. 1997. Partial purification and characterization of manganese-oxidizing factors of *Pseudomonas fluorescens* GB-1. *Appl Environ Microbiol* 63:4793–4799.
 55. Cahyani VR, Murase J, Ishibashi E, Asakawa S, Kimura M. 2009. Phylogenetic positions of Mn²⁺-oxidizing bacteria and fungi isolated from Mn nodules in rice field soils. *Biol Fertil Soils* 45:337–346. <http://dx.doi.org/10.1007/s00374-008-0337-8>.
 56. Palmer FE, Staley JT, Murray RGE, Counsell T, Adams JB. 1986. Identification of manganese-oxidizing bacteria from desert varnish. *Geomicrobiol J* 4:343–360. <http://dx.doi.org/10.1080/01490458609385943>.
 57. Bromfield SM, David DJ. 1976. Sorption and oxidation of manganese ions and reduction of manganese oxide by cell suspensions of a manganese oxidizing bacterium. *Soil Biol Biochem* 8:37–43. [http://dx.doi.org/10.1016/0038-0717\(76\)90019-5](http://dx.doi.org/10.1016/0038-0717(76)90019-5).
 58. Zalar P, de Hoog GS, Schroers HJ, Crous PW, Groenewald JZ, Gunde-Cimerman N. 2007. Phylogeny and ecology of the ubiquitous saprobe *Cladosporium sphaerospermum*, with descriptions of seven new species from hypersaline environments. *Stud Mycol* 58:157–183. <http://dx.doi.org/10.3114/sim.2007.58.06>.
 59. Miyata N, Tani Y, Maruo K, Tsuno H, Sakata M, Iwahori K. 2006. Manganese(IV) oxide production by *Acremonium* sp. strain KR21-2 and extracellular Mn(II) oxidase activity. *Appl Environ Microbiol* 72:6467–6473.
 60. Madigan MT. 2012. Brock biology of microorganisms. Benjamin Cummings/Pearson, San Francisco, CA.
 61. Francis CA, Co EM, Tebo BM. 2001. Enzymatic manganese(II) oxidation by a marine alpha-Proteobacterium. *Appl Environ Microbiol* 67:4024–4029. <http://dx.doi.org/10.1128/AEM.67.9.4024-4029.2001>.
 62. Spilde MN, Northup DE, Boston PJ, Schelble RT, Dano KE, Crossey LJ, Dahm CN. 2005. Geomicrobiology of cave ferromanganese deposits: a field and laboratory investigation. *Geomicrobiol J* 22:99–116. <http://dx.doi.org/10.1080/01490450590945889>.
 63. Northup DE, Barns SM, Yu LE, Spilde MN, Schelble RT, Dano KE, Crossey LJ, Connolly CA, Boston PJ, Natvig DO, Dahm CN. 2003. Diverse microbial communities inhabiting ferromanganese deposits in Lechuguilla and Spider Caves. *Environ Microbiol* 5:1071–1086. <http://dx.doi.org/10.1046/j.1462-2920.2003.00500.x>.
 64. Tyler PA. 1970. *Hyphomicrobia* and the oxidation of manganese in aquatic ecosystems. *Antonie Van Leeuwenhoek* 36:567–578. <http://dx.doi.org/10.1007/BF02069059>.
 65. Green SJ, Prakash O, Gihring TM, Akob DM, Jasrotia P, Jardine PM, Watson DB, Brown SD, Palumbo AV, Kostka JE. 2010. Denitrifying bacteria isolated from terrestrial subsurface sediments exposed to mixed-waste contamination. *Appl Environ Microbiol* 76:3244–3254. <http://dx.doi.org/10.1128/AEM.03069-09>.
 66. Chung AP, Lopes A, Nobre MF, Morais PV. 2010. *Hymenobacter perflusus* sp. nov., *Hymenobacter flocculans* sp. nov., and *Hymenobacter metalli* sp. nov.: three new species isolated from an uranium mine waste water treatment system. *Syst Appl Microbiol* 33:436–443. <http://dx.doi.org/10.1016/j.syapm.2010.09.002>.
 67. Jørgensen SL, Thorseth IH, Pedersen RB, Baumberger T, Schleper C. 2013. Quantitative and phylogenetic study of the Deep Sea Archaeal Group in sediments of the Arctic mid-ocean spreading ridge. *Front Microbiol* 4:299. <http://dx.doi.org/10.3389/fmicb.2013.00299>.
 68. Takai K, Moser DP, DeFlaun M, Onstott TC, Fredrickson JK. 2001. Archaeal diversity in waters from deep South African gold mines. *Appl Environ Microbiol* 67:5750–5760. <http://dx.doi.org/10.1128/AEM.67.21.5750-5760.2001>.
 69. Lehtovirta-Morley LE, Stoecker K, Vilcinskas A, Prosser JI, Nicol GW. 2011. Cultivation of an obligate acidophilic ammonia oxidizer from a nitrifying acid soil. *Proc Natl Acad Sci U S A* 108:15892–15897. <http://dx.doi.org/10.1073/pnas.1107196108>.
 70. Glenn JK, Akileswaran L, Gold MH. 1986. Mn(II) oxidation is the principal function of the extracellular Mn-peroxidase from *Phanerochaete chrysosporium*. *Arch Biochem Biophys* 251:688–696. [http://dx.doi.org/10.1016/0003-9861\(86\)90378-4](http://dx.doi.org/10.1016/0003-9861(86)90378-4).
 71. Schlosser D, Höfer C. 2002. Laccase-catalyzed oxidation of Mn²⁺ in the presence of natural Mn³⁺ chelators as a novel source of extracellular H₂O₂ production and its impact on manganese peroxidase. *Appl Environ Microbiol* 68:3514–3521. <http://dx.doi.org/10.1128/AEM.68.7.3514-3521.2002>.
 72. Rosseinsky DR. 1963. The reaction between mercury(I) and manganese(III) in aqueous perchlorate solution. *J Chem Soc Resumed* 1181–1186.
 73. Tebo BM, Bargar JR, Clement BG, Dick GJ, Murray KJ, Parker D, Verity R, Webb SM. 2004. Biogenic manganese oxides: properties and mechanisms of formation. *Annu Rev Earth Planet Sci* 32:287–328. <http://dx.doi.org/10.1146/annurev.earth.32.101802.120213>.
 74. Ostwald J. 1981. Evidence for a biogeochemical origin of the Grooteylandt manganese ores. *Econ Geol* 76:556–567. <http://dx.doi.org/10.2113/gsecongeo.76.3.556>.
 75. Kiliass SP, Detsi K, Godelitsas A, Typas M, Naden J, Marantos Y. 2007. Evidence of Mn-oxide biomineralization, Vani Mn deposit, Milos, Greece, p 1069–1072. In Andrew CJ (ed), Digging deeper: proceedings of the ninth biennial meeting of the Society for Geology Applied to Mineral Deposits. Irish Association of Economic Geologists, Dublin, Ireland.
 76. McKeown DA, Post JE. 2001. Characterization of manganese oxide mineralogy in rock varnish and dendrites using X-ray absorption spectroscopy. *Am Mineral* 86:701–713. <http://dx.doi.org/10.2138/am-2001-5-611>.
 77. Grote G, Krumbein WE. 1992. Microbial precipitation of manganese by bacteria and fungi from desert rock and rock varnish. *Geomicrobiol J* 10:49–57. <http://dx.doi.org/10.1080/01490459209377903>.
 78. Mayanna S, Peacock CL, Schäffner F, Grawunder A, Merten D, Kothe E, Büchel G. 2015. Biogenic precipitation of manganese oxides and enrichment of heavy metals at acidic soil pH. *Chem Geol* 402:6–17. <http://dx.doi.org/10.1016/j.chemgeo.2015.02.029>.
 79. Turner S, Buseck PR. 1979. Manganese oxide tunnel structures and their intergrowths. *Science* 203:456–458. <http://dx.doi.org/10.1126/science.203.4379.456>.
 80. Burns RG, Burns VM, Stockman HW. 1985. The todorokite-buserite problem: further considerations. *Am Miner* 70:205–208.
 81. Turner S, Buseck PR. 1981. Todorokites: a new family of naturally occurring manganese oxides. *Science* 212:1024–1027. <http://dx.doi.org/10.1126/science.212.4498.1024>.
 82. Toyoda K, Tebo BM. 2013. The effect of Ca²⁺ ions and ionic strength on Mn(II) oxidation by spores of the marine *Bacillus* sp. SG-1. *Geochim Cosmochim Acta* 101:1–11. <http://dx.doi.org/10.1016/j.gca.2012.10.008>.
 83. He J, Zhang L, Jin S, Zhu Y, Liu F. 2008. Bacterial communities inside and surrounding soil iron-manganese nodules. *Geomicrobiol J* 25:14–24. <http://dx.doi.org/10.1080/01490450701829014>.
 84. Beal EJ, House CH, Orphan VJ. 2009. Manganese- and iron-dependent marine methane oxidation. *Science* 325:184–187. <http://dx.doi.org/10.1126/science.1169984>.
 85. Vaughan MJ, Nelson W, Soderlund C, Maier RM, Pryor BM. 2015. Assessing fungal community structure from mineral surfaces in Kartchner caverns using multiplexed 454 pyrosequencing. *Microb Ecol* 70:175–187. <http://dx.doi.org/10.1007/s00248-014-0560-9>.
 86. Weiner S, Dove PM. 2003. An overview of biomineralization processes and the problem of the vital effect. *Rev Mineral Geochem* 54:1–29. <http://dx.doi.org/10.2113/0540001>.
 87. Moy YP, Neilan BA, Foster LJR, Madgwick JC, Rogers PL. 2003. Screening, identification and kinetic characterization of a bacterium for Mn(II) uptake and oxidation. *Biotechnol Lett* 25:1407–1413. <http://dx.doi.org/10.1023/A:1025043326629>.
 88. Ehrlich HL. 1968. Bacteriology of manganese nodules II. manganese oxidation by cell-free extract from a manganese nodule bacterium. *Appl Microbiol* 16:197–202.
 89. Johnson KW, Carmichael MJ, McDonald W, Rose N, Pitchford J, Windelspecht M, Karatan E, Bräuer SL. 2012. Increased abundance of *Gallionella* spp., *Leptothrix* spp., and total bacteria in response to enhanced Mn and Fe concentrations in a disturbed southern Appalachian high elevation wetland. *Geomicrobiol J* 29:124–138. <http://dx.doi.org/10.1080/01490451.2011.558557>.

90. Anderson CR, Davis RE, Bandolin NS, Baptista AM, Tebo BM. 2011. Analysis of in situ manganese(II) oxidation in the Columbia River and offshore plume: linking *Aurantimonas* and the associated microbial community to an active biogeochemical cycle. *Environ Microbiol* 13:1561–1576. <http://dx.doi.org/10.1111/j.1462-2920.2011.02462.x>.
91. Mandernack KW, Post J, Tebo BM. 1995. Manganese mineral formation by bacterial spores of the marine *Bacillus*, strain SG-1: evidence for the direct oxidation of Mn(II) to Mn(IV). *Geochim Cosmochim Acta* 59:4393–4408. [http://dx.doi.org/10.1016/0016-7037\(95\)00298-E](http://dx.doi.org/10.1016/0016-7037(95)00298-E).
92. Anderson CR, Dick GJ, Chu ML, Cho JC, Davis RE, Bräuer SL, Tebo BM. 2009. *Aurantimonas manganooxydans*, sp. nov. and *Aurantimonas litoralis*, sp. nov.: Mn(II) oxidizing representatives of a globally distributed clade of alpha-*Proteobacteria* from the order *Rhizobiales*. *Geomicrobiol J* 26:189–198. <http://dx.doi.org/10.1080/01490450902724840>.
93. Beukes LS, Schmidt S. 2012. Isolation and characterization of a manganese-oxidizing bacterium from a biofiltration system for the treatment of borehole water in KwaZulu-Natal (South Africa). *Eng Life Sci* 12:544–552. <http://dx.doi.org/10.1002/elsc.201100153>.